This article has been accepted for publication in a future issue of this journal, but has not been fully edited. Content may change prior to final publication. Citation information: DOI 10.1109/TSTE.2019.2931670, IEEE Transactions on Sustainable Energy



# Risk-Oriented Multi-Area Economic Dispatch Solution with High Penetration of Wind Power Generation and Compressed Air Energy Storage System

Ali Azizivahed, *Member, IEEE,* Seyed-Ehsan Razavi, Ali Arefi, *Senior Member, IEEE*, Mojtaba Jabbari Ghadi, Li Li, *Member*, *IEEE*, Jiangfeng Zhang, Miadreza Shafie-khah*, Senior Member, IEEE*, and João P. S. Catalão, *Senior Member, IEEE*

***Abstract*—This paper investigates the risk-oriented multi-area economic dispatch (MAED) problem with high penetration of wind farms (WFs) combined with compressed air energy storage (CAES). The main objective is to help system operators to minimize the operational cost of thermal units and CAES units with an appropriate level of security through optimized WF power generation curtailment strategy and CAES charging/discharging control. In the obtained MAED model, several WFs integrated with CAES units are considered in different generation zones, and the probability to meet demand by available spinning reserve during $N-1$ security contingency is characterized as a risk function. Furthermore, the contribution of CAES units in providing the system spinning reserve is taken into account in the MAED model. The proposed framework is demonstrated by a case study using the modified IEEE 40-generator system. The numerical results reveal that the proposed method brings a significant advantage to the efficient scheduling of thermal units' power generation, WF power curtailment and CAES charging/discharging control in the power system.**

***Index Terms*—Multi-Area Economic Dispatch, Compressed Air Energy Storage, Operational Risk, Wind Farm Power Curtailment.**

## NOMENCLATURE

**Indices**

| | |
|---|---|
| $d$ | Demand discrete levels $\epsilon\{1,2,\dots,N_{DL}\}$ |
| $d'$ | Demand discrete levels $\epsilon\{1,2,\dots,N'_{DL}\}$ |
| $i$ | Thermal units $\epsilon\{1,2,\dots,N_{TU}\}$ |
| $j$ | Wind power discrete levels $\epsilon\{1,2,\dots,N_{DW}\}$ |
| $j'$ | Wind power discrete levels $\epsilon\{1,2,\dots,N'_{DW}\}$ |
| $k$ | CAES units $\epsilon\{1,2,\dots,N_{CAES}\}$ |
| $l$ | Tie-lines $\epsilon\{1,2,\dots,N_{TL}\}$ |
| $t$ | Hourly scheduling intervals $\epsilon\{1,2,\dots,24\}$ |
| $w$ | Wind farms $\epsilon\{1,2,\dots,N_{WF}\}$ |
| $n$ | Power system separated areas |
| $m$ | The auxiliary indices for merging $\epsilon\{1,2,\dots,N_{DL}+N'_{DL}-1\}$ |
| $m'$ | The auxiliary indices for merging $\epsilon\{1,2,\dots,N_{DW}+N'_{DW}-1\}$ |
| $m''$ | The auxiliary indices for merging $\epsilon\{1,2,\dots,N_{DW}+N_{DL}+N'_{DW}+N'_{DL}-3\}$ |

**Vectors**

| | |
|---|---|
| $\boldsymbol{C}^{w}$ | The curtailment level of $w^{th}$ WF for 24-hour timespan |
| $\boldsymbol{P}^{l}_{TL}$ | Set of amount of power flow of the $l^{th}$ tie-line for 24-hour time scheduling |
| $\boldsymbol{P}^{i}_{TU}$ | Set of amount of power generation of $i^{th}$ thermal unit for 24-hour time scheduling |
| $\boldsymbol{P}^{k}_{ch/dis}$ | Set of amount of charge/discharge power of the $k^{th}$ CAES for 24-hour time scheduling |
| $\boldsymbol{P}^{t}_{Dr}$ | The residual demand at $t^{th}$ hour |
| $\boldsymbol{P}^{n,t}_{D}$ | The power consumption of $n^{th}$ area at $t^{th}$ hour |
| $\boldsymbol{P}^{t}_{D}$ | The total power consumption of the system |
| $\boldsymbol{\pi}^{n,t}_{D}$ | The PDF of the demand at $n^{th}$ area |
| $\boldsymbol{\pi}^{t}_{D}$ | The PDF of the merged demand |
| $\boldsymbol{P}^{w,t}_{WT}$ | The active power generation by $w^{th}$ wind |
| $\overline{\boldsymbol{P}}^{w,t}_{WT}$ | The set of curtailed power generation of $w^{th}$ wind farm at $t^{th}$ hour |
| $\overline{\boldsymbol{\pi}}^{w,t}_{WT}$ | The PDF of curtailed power generation of $w^{th}$ wind farm at $t^{th}$ hour |
| $\boldsymbol{X}_{CAES}$ | CAES decision variables sub-vector |
| $\boldsymbol{X}_{TL}$ | Tie-line decision variables sub-vector |
| $\boldsymbol{X}_{TU}$ | Thermal unit decision variables sub-vector |
| $\boldsymbol{X}_{WFC}$ | WF power generation curtailment level unit decision variables sub-vector |

**Objective functions**

| | |
|---|---|
| $F_{Tech}$ | Technical function |
| $F_{Opr}$ | Operational function |
| $\widetilde{F_{Opr}}$ | Normalized operational function |
| $F_{Risk}$ | Risk function |
| $F^{Max}_{Opr}$ | Maximum operational cost |
| $F^{Min}_{Opr}$ | Minimum operational cost |

**Flags**

| | |
|---|---|
| $TU^{i,t}_{Violate}$ | The violation flag for the $i^{th}$ thermal unit |
| $TL^{l,t}_{Violate}$ | The violation flag for the $l^{th}$ tie-lines limitation |
| $PB^{t}_{Violate}$ | The violation flag for the power balance constraint |
| $CAES^{k,t}_{Violate}$ | The violation flag for $k^{th}$ CAES unit operation |

**Coefficients**

| | |
|---|---|
| $a_i, b_i, c_i$ | The cost coefficients of the $i^{th}$ thermal unit |
| $\xi^{w}_{O\&M}$ | The operation & maintenance cost of the $w^{th}$ WF |
| $\Psi^{dis,k}(\Psi^{s,k})$ | The heat ratio of the $k^{th}$ CAES for discharging (simple cycle) mode |
| $\varphi_{NG}$ | The gas price of the CAES units |
| $Vc^{k}_{Exp}, (Vc^{k}_{Com})$ | The variable operation and maintenance cost for expanding (compressing) modes of the $k^{th}$ CAES |

This work was partially funded by Murdoch University, Western Australia Australia. Moreover, J.P.S. Catalão acknowledges the support by FEDER funds through COMPETE 2020 and by Portuguese funds through FCT, under POCI-01-0145-FEDER-029803 (02/SAICT/2017). (*Corresponding authors: Miadreza Shafie-khah and João P. S. Catalão*).

A. Azizivahed, M. Jabbary, L. Li and J. Zhang are with the Faculty of Engineering and Information Technology, University of Technology Sydney, PO Box 123, Broadway, NSW 2007, Australia (Emails: {Ali.Azizivahed, mojtaba.jabbarighadi}@student.uts.edu.au; {li.li,Jiangfeng.zhang}@uts.edu.au).

S-E. Razavi and A. Arefi are with Discipline of Engineering and Energy, College of Science, Health, Engineering and Education, Murdoch University, Western Australia 6150, Australia (Emails: {ehsan.razavi,ali.arefi}@murdoch.edu.au).

M. Shafie-khah is with the School of Technology and Innovations, University of Vaasa, 65200 Vaasa, Finland (e-mail: mshafiek@univaasa.fi).

J.P.S. Catalão is with the Faculty of Engineering of the University of Porto and INESC TEC, Porto 4200-465, Portugal (e-mail: catalao@fe.up.pt).

This article has been accepted for publication in a future issue of this journal, but has not been fully edited. Content may change prior to final publication. Citation information: DOI 10.1109/TSTE.2019.2931670, IEEE Transactions on Sustainable Energy



| | |
|---|---|
| $\rho^{ch,k}, \rho^{dis,k}$ | The charge and discharge energy ratio for converting power to energy in $k^{th}$ CAES cavern |
| $FOR_{TU}^{i}$ | The forced outage rate of the $i^{th}$ thermal unit |
| $\beta$ | The weighting factor |
| 0 | A large number (i.e $10^{10}$) |
| **Parameters** | |
| $C^{w,t}$ | Curtailment level of $w^{th}$ WF at $t^{th}$ hour $\epsilon \boldsymbol{C}^{w}$ |
| $P_{TU}^{i,t}$ | Active power generated by $i^{th}$ thermal unit |
| $P_{ch}^{k,t}(P_{dis}^{k,t})$ | Charging (discharging) power of the $k^{th}$ CAES unit |
| $P_{c}^{k,t}$ | The power generation of the $k^{th}$ CAES unit at $t^{th}$ hour in the simple cycle mode |
| $\pi_{risk}^{t}$ | The risk index at $t^{th}$ hour |
| $P_{TU_{max}}^{i}(P_{TU_{min}}^{i})$ | Maximum(minimum) capacity of $i^{th}$ thermal unit |
| $RU^{i}, RL^{i}$ | Ramp-up and ramp-down rate of $i^{th}$ thermal unit |
| $P_{TL}^{l,t}$ | Active power flow of $l^{th}$ Tie-line at $t^{th}$ hour |
| $P_{TL_{max}}^{l}$ | Maximum capacity of $l^{th}$ Tie-line |
| $E_{CAES}^{k,t}$ | Amount of energy inside the $k^{th}$ CAES unit |
| $E_{CAES_{max}}^{k}$ $(E_{CAES_{min}}^{k})$ | Maximum(minimum) limit of the amount of energy inside the $k^{th}$ CAES unit |
| $P_{ch/dis_{max}}^{k}$ | Maximum permitted of charging/discharging rate for the $k^{th}$ CAES unit |
| $\pi_{Reserve}^{t,m''}$ | The probability of difference between residual demand and the expected value lying between up and down spinning reserves |
| $P_{Dr}^{expt,t}$ | Expected value of residual demand at $t^{th}$ hour |
| $SR_{Up}^{t}, SR_{Dn}^{t}$ | Up and down system spinning reserve |
| $\pi_{D}^{n,t,d}$ | Probability of demand of $n^{th}$ area for $d^{th}$ discrete level |
| $P_{D}^{n,t,d}$ | The demand of $n^{th}$ area for $d^{th}$ discrete level at $t^{th}$ hour $\epsilon \boldsymbol{P}_{D}^{n,t}$ |
| $P_{D}^{t,m}$ | Demand of network for $m^{th}$ discrete level |
| $\bar{P}_{WT}^{t,m'}$ | Curtailed power generation of network at $m'^{th}$ discrete |
| $\bar{P}_{WT}^{w,t,j}$ | The curtailed power generation of $w^{th}$ wind farm at $j^{th}$ discrete level at $t^{th}$ hour $\epsilon \bar{\boldsymbol{P}}_{WT}^{w,t}$ |
| $\pi_{WT}^{w,t,j}$ | The probability of power generation of $w^{th}$ wind farm for $j^{th}$ discrete level at $t^{th}$ hour |
| $\bar{\pi}_{WT}^{w,t,j}$ | The probability of curtailed power generation of $w^{th}$ wind farm for $j^{th}$ discrete level at $t^{th}$ hour |
| $\bar{\pi}_{WT}^{t,m'}$ | The probability of curtailed WF power generation of network for $m'^{th}$ discrete level at $t^{th}$ hour |
| $\pi_{Dr}^{t,m''}$ | The probability of residual demand of network for $m''^{th}$ discrete level at $t^{th}$ hour |

## I. Introduction

Wind power generation has markedly increased over the past decade. However, its intermittent nature poses a serious obstacle to utilize its supplied energy in a reliable way. Accordingly, a lot of studies have been carried out to optimally manage wind energy, in which energy storages play a decisive role in the management of such a renewable energy source (RES). In a system with high penetration of wind energy, bulk energy storage enables a reliable power dispatch.

In particular, compressed air energy storage (CAES) can be an effective solution at utility scales, which could have capacities of several hundred MW and be constructed within three years [1]. CAES has not only positive effects on power system performance [2], but also plays an active role in meeting the heating loads as a subsidiary benefit when it comes to selling of compression waste heat during waste heat recovery process, for instance, both adiabatic and distributed CAES can improve the efficiency associated with waste heat of the compressor [3].

Integration of CAES and wind-thermal scheduling has been investigated for single area analysis. For example, references [4-6] develop a deterministic framework for scheduling where wind is not considered as a source of uncertainty. The authors of [4] have optimized the short-term generation of wind and conventional gas-fired units in the presence of CAES while considering technical limitations such as ramp rates and minimum on/off time.

A market-based self-scheduling approach has been proposed in [5] where the thermodynamic characteristics of CAES has been taken into account. Furthermore, a new integration of CAES and combined cooling, heating and power (CCHP) system has been developed in [6] to meet electrical, cooling and heating loads in peak hours. Ghalelou et al. [7] have presented a stochastic model for scheduling of CAES coupled with RESs and thermal plants while an effective demand response program has been used to flatten the load curve, leading to lower operational cost. It is noteworthy that the above-mentioned publications have ignored the transmission and/or tie lines power flow limits, since a single-area economic dispatch (ED) model is applied there which cannot demonstrate the real vision and the economic solution for short-term scheduling for interconnected areas. To fill this gap, multi-area ED (MAED) has been well addressed through studies in [8-10].

Furthermore, to consider capacity limits for all network lines, security-constrained unit commitment (SCUC) has been solved while wind power generation is included [11, 12]. In this regard, [11] proposes a new probabilistic SCUC for wind-thermal units to find the optimal solution with respect to the cost of energy and expected energy not supplied. Also, CAES is also included into the SCUC model in [12] to investigate the effect of this kind of storage on peak load shaving and locational market, while wind and demand load are considered as deterministic inputs. However, all these works provide a deterministic formulation, not considering the risk associated with load and wind generation uncertainties.

Deployment of RESs as well as variation of demand and RESs require studies on the risk associated with these uncertain sources [13]. In an ordinary generation schedule where risks are not considered, the main attention is to achieve the minimum operational cost under technical constraints of units and other assets. While in a risk-oriented generation schedule, additional emphasis is on including operational risk of unit failures in addition to other uncertainties. Indeed, a risk-based scheduling strategy allows system operators to make a compromise between costs of generation and those of uncertainties [14]. In this regard, an optimal risk-based strategy for wind-thermal unit commitment (UC) has been proposed in [15] for market clearing. Reference [15] has considered the risks of loss of load, branch capacity and wind curtailment. In [16], a heuristic approach has been presented to solve multi-objective wind-thermal UC, in which one of the objectives is operational cost and the other is the risks associated with generation outage and wind curtailment.

This article has been accepted for publication in a future issue of this journal, but has not been fully edited. Content may change prior to final publication. Citation information: DOI 10.1109/TSTE.2019.2931670, IEEE Transactions on Sustainable Energy



To take advantage of bulk energy storages as a potential factor to mitigate wind fluctuations, a few studies have been concentrated on the risk evaluation in a wind integrated system coupled with CAES. For instance, [17] has developed an optimal scenario-based look-ahead scheduling in the wind integrated network with CAES, where the conditional value at risk (CVaR) index has been deployed to include the risk related to wind, demand and price.

Apart from the risk of wind availability, similar risk due to market price has been investigated in [18] to present an optimal offering strategy in a wind integrated system with CAES. Though the presented robust strategy in [18] considers the uncertain price, wind generation is treated deterministically based on a fix prediction.

In a power system with high penetration of wind generation, the issue of wind curtailment is a prevalent and practical solution of ED to the system operators, especially when the system technical constraints are on the verge of violation [19]. Regarding the valuable works reviewed above on the short-term scheduling of wind-thermal plants integrated with CAES, there is still a need for a comprehensive and optimal framework in which the risk of meeting demand due to wind and load uncertainties are taken into account, taking advantage of two effective tools, that are wind power generation curtailment and possibility of providing spinning reserve by CAES.

Accordingly, this paper aims to bridge the gap mentioned by proposing an optimal comprehensive management model. The model should give operators a decision-making strategy in which the most ED can be achieved by proper wind power generation curtailment as well as optimal CAES charging and discharging control to provide the required spinning reserve with respect to outages of the single thermal unit. Eventually, the problem can be completed when the constraints related to the several generation zones are considered through a MAED problem. To address the above-mentioned problem, this paper presents a risk-oriented management scheme.

Overall, the main contributions of this paper are summarized as follows:

- Optimal MAED strategy in power systems with high penetration of wind and CAES under technical constraints associated with different generation zones;
- A risk-based model to cope with the uncertainties of wind generation and load with respect to $N-1$ contingency;
- A decision-making method for system operators with respect to the optimal solution of wind-thermal ED, intentional wind power generation curtailment and CAES deployment, while spinning reserve provided by thermal and CAES units is taken into account;
- A method for working with different and independent probability distribution functions (PDFs) of wind and load corresponding to the different generation zones. It is worth mentioning that this issue makes the problem much more sophisticated compared with ordinary single area ED.

The remainder of this paper is organized as follows. Section II presents the proposed mathematical formulation. Numerical studies are discussed in Section III, and conclusions are drawn in Section IV.

## II. Mathematical Modeling

This section provides a mathematical model for a 24-hour scheduling of thermal units, WF and CAES operation in multiple areas where some of the main assumptions of the proposed problem will be power system configuration, different load profiles and PDFs of wind for each generation area, cost coefficients of each generation units and forced outage rate (FOR) of thermal units. Also, the decision variable vector, objective function, uncertainty modeling and WF power generation curtailment are formulated. The problem is defined as a mix-integer non-linear programming (MINLP) problem as follows.

*Decision Variables*:

In this problem, the main decision variable vector consists of several sub-vectors including thermal unit power generation, power flow through the tie-lines, WF power generation curtailing level and CAES units' charging/discharging schedule.

$$\boldsymbol{X} = [\boldsymbol{X}_{TU} \quad \boldsymbol{X}_{TL} \quad \boldsymbol{X}_{Wc} \quad \boldsymbol{X}_{CAES}] \tag{1}$$

$$\boldsymbol{X}_{TU} = \left[\boldsymbol{P}_{TU}^{1} \quad \boldsymbol{P}_{TU}^{2} \quad \dots \quad \boldsymbol{P}_{TU}^{N_{TU}}\right], \quad \boldsymbol{P}_{TU}^{i} \in \mathbb{R}^{1\times 24} \tag{2}$$

$$\boldsymbol{X}_{TL} = \left[\boldsymbol{P}_{TL}^{1} \quad \boldsymbol{P}_{TL}^{2} \quad \dots \quad \boldsymbol{P}_{TL}^{N_{TL}}\right], \quad \boldsymbol{P}_{TL}^{l} \in \mathbb{R}^{1\times 24} \tag{3}$$

$$\boldsymbol{X}_{WFC} = [\boldsymbol{C}^{1} \quad \boldsymbol{C}^{2} \quad \dots \quad \boldsymbol{C}^{N_{WF}}], \quad \boldsymbol{C}^{w} \in \mathbb{Z}^{1\times 24} \tag{4}$$

$$\boldsymbol{X}_{CAES} = \left[\boldsymbol{P}_{ch/dis}^{1} \; \boldsymbol{P}_{ch/dis}^{2} \; \dots \; \boldsymbol{P}_{ch/dis}^{N_{CAES}}\right], \quad \boldsymbol{P}_{ch/dis}^{k} \in \mathbb{R}^{1\times 24} \tag{5}$$

*WF Curtailment:*

WF power generation curtailment is a mechanism to restrain the percentage of WF power generation uncertainty by controlling the blade pitch angle.

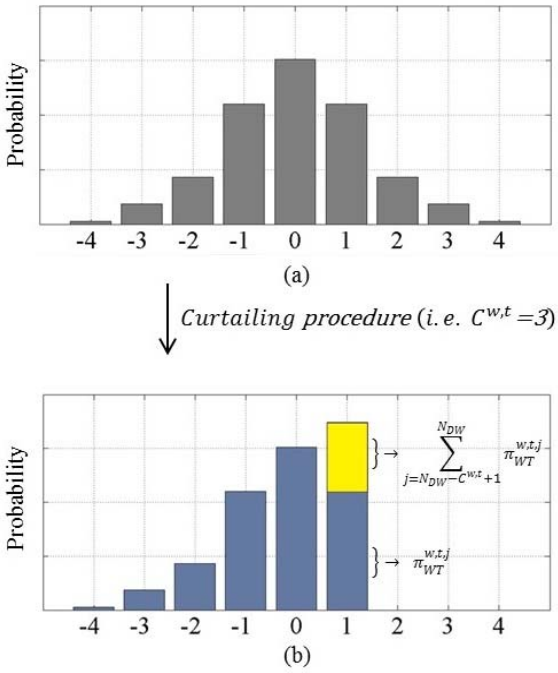


Fig. 1 (a) The original WF power generation PDF, (b) the post-curtailment WF power generation PDF

This article has been accepted for publication in a future issue of this journal, but has not been fully edited. Content may change prior to final publication. Citation information: DOI 10.1109/TSTE.2019.2931670, IEEE Transactions on Sustainable Energy



This mechanism brings many advantages such as providing an appropriate wind-thermal economic dispatch with high penetration of WF and reducing the portion of uncertain WF power generation. The forecast WF power generation is assumed as a normal PDF and is discretized into $N_{DW}$ levels with different standard deviation at each hour. By applying the specific level of WF power generation curtailment, the mentioned PDF is reshaped as follows (6). [19]:

$$\bar{\pi}_{WT}^{w,t,j} = \begin{cases} \pi_{WT}^{w,t,j} & 1 \le j < N_{DW} - C^{w,t} \\ \sum_{j=N_{DW}-C^{w,t}}^{N_{DW}} \pi_{WT}^{w,t,j} & j = N_{DW} - C^{w,t} \\ 0 & N_{DW} - C^{w,t} < j \end{cases} \quad (6)$$

As it is clear from (6), the higher curtailment level ($C^{w,t}$), the lower wind power generation, and vice versa. To better understand the curtailing procedure, a representative example is presented here. According to Fig. 1(a), if the original PDF associated with a WF power generation is discretized into nine levels, $N_{DW} = 9$, the reshaped PDF considering a six-level curtailment ($C^{w,t} = 3$) will be obtained as Fig. 1(b).

*Objective Function and Constraints:*

The objective function of the proposed problem is formulated as (7) including three terms to consider operational cost (8)-(9), operational risk (10) and technical constraints (11), respectively. Moreover, the weighted sum method is used in this objective function to make a trade-off between operational cost and risk function.

$$Min\ Obj = \beta.\widehat{F_{Opr}}(\boldsymbol{X}) + (1-\beta).F_{Risk}(\boldsymbol{X}) + F_{Tech}(\boldsymbol{X}) \quad (7)$$

The operational cost stated in the first term of the objective function is expanded in (8).

$$F_{Opr}(\boldsymbol{X}) = \sum_{t=1}^{24}\left(\sum_{i=1}^{N_{TU}}\left(a_i P_{TU}^{i,t\,2} + b_i P_{TU}^{i,t} + c_i\right) + \sum_{w=1}^{N_{WF}}\left(\xi_{O\&M}^{w} P_{WT}^{w,t}\right) + \sum_{k=1}^{N_{CAES}}\begin{pmatrix} P_{dis}^{k,t}\left(\Psi^{dis,k}\varphi_{NG} + Vc_{Exp}^{k}\right) + \\ P_{s}^{k,t}\left(\Psi^{s,k}\varphi_{NG} + Vc_{Exp}^{k} + Vc_{Com}^{k}\right) + P_{ch}^{k,t} Vc_{Com}^{k} \end{pmatrix}\right) \quad (8)$$

Based on the proposed model, the cost comprises three main factors related to fuel cost of thermal units, operational and maintenance cost of wind farms and operational cost of CAES units that are respectively formulated in the first to the third terms of (8). In more detail, the major operational cost involved in CAES consists of the charging and discharging modes which, indeed, correspond to expanding and compressing processes. These considerations have been formulated through the third term of (8). The term "$P_{ch}^{k,t} Vc_{Com}^{k}$" in (8) relates to the technology of CAES that enables it to work as a gas turbine, named simple-cycle [18, 20, 21]. On the other hand, the proposed risk function ($F_{Risk}$), lies between zero and one due to the concept of probability used, i.e. $0 \le F_{Risk} \le 1$. Thus, the operational function ($F_{Opr}$) is required to be normalized. In this regard, the fuzzy technique is implemented as in (9). It should be noted that $F_{Opr}^{Max}$ is assumed to be equal to $10 \times F_{Opr}^{Min}$.

$$\widehat{F_{Opr}}(\boldsymbol{X}) = \frac{F_{Opr}^{Max} - F_{Opr}(X)}{F_{Opr}^{Max} - F_{Opr}^{Min}} \quad (9)$$

The second term of the objective function discusses the risk associated with the problem as in (10) which will be addressed later through (17)–(20).

$$F_{Risk}(\boldsymbol{X}) = \frac{1}{24}\sum_{t=1}^{24} \pi_{risk}^{t} \quad (10)$$

The problem constraints are mentioned in the third term of (7) are handled using penalty factor in the objective function through (11). To observe these constraints, (12)-(16) need to be deployed.

$$F_{Tech}(\boldsymbol{X}) = \sum_{t=1}^{24}\left(\begin{matrix} PB_{Violate}^{t} + \sum_{i=1}^{N_{TU}} TU_{Violate}^{i,t} \\ + \sum_{l=1}^{N_{TL}} TL_{Viovate}^{l,t} + \sum_{k=1}^{N_{CAES}} CAES_{Violate}^{k,t} \end{matrix}\right) \times \mathcal{M} \quad (11)$$

$$TU_{Violate}^{i,t} = \begin{cases} 0 & P_{TU_{min}}^{i} \le P_{TU}^{i,t} \le P_{TU_{max}}^{i} \ \& \\ & RL^{i} \le P_{TU}^{i,t} - P_{TU}^{i,t-1} \le RU^{i} \\ 1 & otherwise \end{cases}, \forall i,t \quad (12)$$

$$TL_{Viovate}^{l,t} = \begin{cases} 0 & \left|P_{TL}^{l,t}\right| \le P_{TL_{max}}^{l} \\ 1 & otherwise \end{cases}, \forall l,t \quad (13)$$

$$PB_{Violate}^{t} = \begin{cases} 0 & \sum_{i=1}^{N_{TU}} P_{TU}^{i,t} + \sum_{w=1}^{N_{WF}} P_{WT}^{w,t} + \sum_{k=1}^{N_{CAES}} P_{ch/dis}^{k,t} = \sum_{n=1}^{N_{Area}} P_{D}^{n,t} \\ 1 & otherwise \end{cases}, \forall t \quad (14)$$

$$CAES_{Violate}^{k,t} = \begin{cases} 0 & \begin{matrix} E_{CAES_{min}}^{k} \le E_{CAES}^{k,t} \le E_{CAES_{max}}^{k} \ \& \\ \left|P_{ch/dis}^{k,t}\right| \le P_{ch/dis_{max}}^{k} \ \& \\ E_{CAES}^{k,1} = E_{CAES}^{k,24} \end{matrix} \\ 1 & otherwise \end{cases}, \forall k,t \quad (15)$$

$$E_{CAES}^{k,t} = E_{CAES}^{k,t-1} + \rho^{ch,k} P_{ch}^{k,t} - \frac{1}{\rho^{dis,k}} P_{dis}^{k,t}, \forall t,k \quad (16)$$

In (12), min/max capacities of the thermal units as well as their up/down ramp rate constraints are taken into account. Constraint (13) guarantees that the tie-lines' power flows are within permitted limits. Power balance constraint, regarding thermal units and wind power generation as well as CAES, is handled by (14). Eqs. (15)-(16) are the limitations due to CAES utilization [17].

Constraint (15) implies that the rate of charge/discharge and the dynamics of the energy stored in the CAES at each hour should be within the permitted range. This amount can be obtained from (16) [18]. It is worth mentioning that the technical function ($F_{Tech}$) can take two values, either zero providing all technical constraints are satisfied or $\mathcal{M}$ when the penalty factor is applied. Obviously, the optimization trend pushes the technical function to be zero as a result of the applied large penalty factor for this constraint. Hence, there is no need to give this term a weighting factor in the objective function.

This article has been accepted for publication in a future issue of this journal, but has not been fully edited. Content may change prior to final publication. Citation information: DOI 10.1109/TSTE.2019.2931670, IEEE Transactions on Sustainable Energy



Indeed, the used penalty factor technique integrated in the objective function is a straightforward way to handle the proposed problem's constraints rather than utilizing hard constraints disallowing violations. By applying the penalty factor technique, satisfying the problem constraints would be the priority; once they are met, the first two remaining terms of objective function is minimized. Operational risk arising from the problem uncertainties, here wind power generation and demand, is formulated in (10). Indeed, the operational risk function in (10) aims at minimizing the risk index of each hour, ($\pi^t_{risk}$,) over the studied horizon which is defined as bellow in (17).

$$\pi^t_{risk} = 1 - \sum_{i=1}^{N_{TU}} \sum_{m''} FOR^i_{TU} \times \pi^{t,m''}_{Reserve} \quad ,\forall t \tag{17}$$

In the context of $N-1$ security criterion of thermal units, the hourly risk index is expressed as in (17) indicating the risk of not supplied demand that stems from the uncertainties of load and wind as well as thermal unit outages, which are not covered by spinning reserve of the system. In other words, the risk is defined as uncertain power generation or demand that is not covered by the reserves. Accordingly, the probability that shows the demand can be met by spinning reserve is calculated in (18).

$$\pi^{t,m''}_{Reserve} = \begin{cases} \pi^{t,m''}_{Dr} & SR^t_{Dn} \le P^{t,m''}_{Dr} - P^{expt,t}_{Dr} \le SR^t_{Up} \quad \forall t\,, m'' \\ 0 & otherwise \end{cases} \tag{18}$$

In this study, the wind power is treated as a negative demand and therefore the difference of demand and power generation is known as residual demand ($P^{t,m''}_{Dr}$). Eq. (18) demonstrates that the uncertainty coverage can be accomplished when the difference between residual demand and the expected value lies between up and down values of spinning reserves. The spinning reserve of the system in similar studies is provided only by means of thermal units.

However, in this paper, the system up and down spinning reserves are affected by CAES along with thermal units. In this regard, up and down spinning reserve of the system are indicated in (19) and (20), respectively.

$$SR^t_{Up} = \sum_{i=1}^{N_{TU}} min\left(P^i_{TU_{max}} - P^{i,t}_{TU}, 10RU^i\right) + \sum_{k=1}^{N_{CAES}} min\left(\frac{\left(E^{k,t-1}_{CAES} - E^k_{CAES_{min}}\right)}{Er^k}, P^k_{ch/dis_{max}}\right) \quad ,\forall t \tag{19}$$

$$SR^t_{Dn} = \sum_{i=1}^{N_{TU}} min\left(P^{i,t}_{TU} - P^i_{TU_{min}}, 10RL^i\right) + \sum_{k=1}^{N_{CAES}} min\left(\frac{\left(E^k_{CAES_{max}} - E^{k,t-1}_{CAES}\right)}{Er^k}, P^k_{ch/dis_{max}}\right) \quad ,\forall t \tag{20}$$

*Dealing with Uncertainties in Different Generation Zones −the Discrete Convolution Technique*

Consideration of different generation zones imposes new challenges to the underlying optimization problem. Though the technical constraint associated with tie-line capacities has already been handled through (13), implementation of a more accurate model for PDFs is of great importance. In reality, it is possible for different zones to have independent PDFs of demand and wind. In the proposed model, it is assumed that different generation areas are far from each other and have independent demand and wind PDFs. Similarly, wind PDFs of different zones are most likely different. Hence, the residual demand and its expected value stated in (18) need to be defined and formulated to encompass the equivalent values for different zones, precisely. Therefore, one equivalent PDF for demand and one for wind are required. To serve this purpose, this paper utilizes the discrete convolution technique to merge the independent PDFs (PDF of each area) [22]. In the following, the detailed modeling of the uncertainties for different areas is presented.

There are several load consumptions and WFs in different areas. The forecasted demand and WF power generation are modeled by normal PDFs discretized into $N_{DL}$ and $N_{DW}$ levels, respectively. In order to calculate the equivalent residual demand ($\boldsymbol{P}^t_{Dr}$), its probability ($\boldsymbol{\pi}^t_{Dr}$) and also its expected value ($P^{expt,t}_{Dr}$) in (18), it is required to merge all load consumptions in all areas together and all curtailed WF power generation as well based on (21)-(27) as below [22].

$$\boldsymbol{P}^t_D = \sum_{n=1}^{N_{Area}} \boldsymbol{P}^{n,t}_D = \left(\dots\left(\left(\boldsymbol{P}^{1,t}_D \oplus \boldsymbol{P}^{2,t}_D\right) \oplus \dots \boldsymbol{P}^{n,t}_D\right) \oplus \dots \boldsymbol{P}^{N_{Area},t}_D\right)$$

$$s.t. \begin{cases} P^{t,m}_D = P^{n-1,t,d}_D + P^{n,t,d'}_D & ,\forall t, m, d, d' \\ & m = N'_{DL} + d - d' \\ P^{n-1,t,d}_D \epsilon\, \boldsymbol{P}^{n-1,t}_D & ,\forall d \\ P^{n,t,d'}_D \epsilon\, \boldsymbol{P}^{n,t}_D & ,\forall d' \\ P^{t,m}_D \epsilon \left\{\boldsymbol{P}^{n-1,t}_D \oplus \boldsymbol{P}^{n,t}_D\right\} & ,\forall m \end{cases} \tag{21}$$

$$\boldsymbol{\pi}^t_D = \bigwedge_{n=1}^{N_{Area}} \boldsymbol{\pi}^{n,t}_D = \left(\dots\left(\left(\boldsymbol{\pi}^{1,t}_D * \boldsymbol{\pi}^{2,t}_D\right) * \dots \boldsymbol{\pi}^{n,t}_D\right) * \dots \boldsymbol{\pi}^{N_{Area}-1,t}_D\right) * \boldsymbol{\pi}^{N_{Area},t}_D$$

$$s.t. \begin{cases} \pi^{t,m}_D = \sum_{m=N'_{DL}+d-d'} \pi^{n-1,t,d}_D \pi^{n,t,d'}_D & ,\forall t, d, d' \\ \pi^{n-1,t,d}_D \epsilon\, \boldsymbol{\pi}^{n-1,t}_D & ,\forall d \\ \pi^{n,t,d'}_D \epsilon\, \boldsymbol{\pi}^{n,t}_D & ,\forall d' \\ \pi^{t,m}_D \epsilon \left\{\boldsymbol{\pi}^{n-1,t}_D * \boldsymbol{\pi}^{n,t}_D\right\} & ,\forall m \end{cases} \tag{22}$$

Eqs. (21)-(22) show the process of merging all the demands together. For better understanding, the mathematical process of merging two demands (i.e. $\boldsymbol{P}^{n-1,t}_D$ and $\boldsymbol{P}^{n,t}_D$) from two different areas (i.e. areas $n-1$ and $n$) and their corresponding probabilities (i.e. $\boldsymbol{\pi}^{n-1,t}_D$ and $\boldsymbol{\pi}^{n,t}_D$) is expressed in these equations.

The discrete convolution technique in (22) is used to calculate the equivalent PDF of the merged loads. Note that the operator ($\oplus$) denotes the sum of two uncertainty variables and the convolution operator used in this equation is denoted by the star symbol (*).

Similarly, Eqs. (23)-(24) are deployed for the uncertainties posed by wind power generation as follows.

$$\overline{\boldsymbol{P}}^t_{WT} = \sum_{w=1}^{N_{WF}} \overline{\boldsymbol{P}}^{w,t}_{WT} = \left(\dots\left(\left(\overline{\boldsymbol{P}}^{1,t}_{WT} \oplus \overline{\boldsymbol{P}}^{2,t}_{WT}\right) \oplus \dots \overline{\boldsymbol{P}}^{w,t}_{WT}\right) \oplus \dots \overline{\boldsymbol{P}}^{N_{WF},t}_{WT}\right) \tag{23}$$

This article has been accepted for publication in a future issue of this journal, but has not been fully edited. Content may change prior to final publication. Citation information: DOI 10.1109/TSTE.2019.2931670, IEEE Transactions on Sustainable Energy



$$s.t.\begin{cases} \bar{P}_{WT}^{t,m'} = \bar{P}_{WT}^{w-1,t,j} + \bar{P}_{WT}^{w,t,j'} & ,\forall t,m',j,j' \\ & m' = N'_{DL} + j - j' \\ \bar{P}_{WT}^{w-1,t,j} \epsilon\, \bar{\boldsymbol{P}}_{WT}^{w-1,t} & ,\forall j \\ \bar{P}_{WT}^{w,t,j'} \epsilon\, \bar{\boldsymbol{P}}_{WT}^{w,t} & ,\forall j' \\ \bar{P}_{WT}^{t,m'} \epsilon \{\bar{\boldsymbol{P}}_{WT}^{w-1,t} \oplus \bar{\boldsymbol{P}}_{WT}^{w,t}\} & ,\forall m' \end{cases}$$

$$\bar{\boldsymbol{\pi}}_{WT}^{t} = \bigwedge_{w=1}^{N_{WF}} \bar{\boldsymbol{\pi}}_{WT}^{w,t} = \left(\ldots \left(\left(\bar{\boldsymbol{\pi}}_{WT}^{1,t} * \bar{\boldsymbol{\pi}}_{WT}^{2,t}\right) * \ldots \bar{\boldsymbol{\pi}}_{WT}^{w,t}\right) * \ldots \bar{\boldsymbol{\pi}}_{WT}^{N_{WF}-1,t}\right) * \bar{\boldsymbol{\pi}}_{WT}^{N_{WF},t}$$

$$s.t.\begin{cases} \bar{\pi}_{WT}^{t,m'} = \sum_{m'=N'_{WT}+j-j'} \bar{\pi}_{WT}^{w-1,t,j} \bar{\pi}_{WT}^{w,t,j'} & ,\forall t,j,j' \\ \bar{\pi}_{WT}^{w-1,t,j} \epsilon\, \bar{\boldsymbol{\pi}}_{WT}^{w-1,t} & ,\forall j \\ \bar{\pi}_{WT}^{w,t,j'} \epsilon\, \bar{\boldsymbol{\pi}}_{WT}^{w,t} & ,\forall j' \\ \bar{\pi}_{WT}^{t,m'} \epsilon \{\bar{\boldsymbol{\pi}}_{WT}^{w-1,t} * \bar{\boldsymbol{\pi}}_{WT}^{w,t}\} & ,\forall m' \end{cases} \quad (24)$$

Eventually, the final equivalent power generation (i.e. $\bar{\boldsymbol{P}}_{WT}^{t}$ with the PDF $\bar{\boldsymbol{\pi}}_{WT}^{t}$) is treated as the negative load consumption in (25) to achieve the residual demand $\boldsymbol{P}_{Dr}^{t}$.

$$\boldsymbol{P}_{Dr}^{t} = \boldsymbol{P}_{D}^{t} \ominus \bar{\boldsymbol{P}}_{WT}^{t} \quad ,\forall t$$

$$s.t.\begin{cases} P_{Dr}^{t,m''} = P_{D}^{t,m} - \bar{P}_{WT}^{t,m'} & ,\forall t,m'',m',m \ \ \& \\ & m'' = N_{DW} + N'_{DW} - 1 + m - m' \\ P_{D}^{t,m} \epsilon\, \boldsymbol{P}_{D}^{t} & ,\forall m \\ \bar{P}_{WT}^{t,m'} \epsilon\, \bar{\boldsymbol{P}}_{WT}^{t} & ,\forall m' \\ P_{Dr}^{t,m''} \epsilon \boldsymbol{P}_{Dr}^{t} & ,\forall m'' \end{cases} \quad (25)$$

Again, by applying the discrete convolution technique, the probability of PDF of the residual demand is obtained by (26). Note that the operator ($\ominus$) denotes the difference of two uncertainty variables.

$$\boldsymbol{\pi}_{Dr}^{t} = \boldsymbol{\pi}_{D}^{t} * \bar{\boldsymbol{\pi}}_{WT}^{t}$$

$$s.t.\begin{cases} \pi_{Dr}^{t,m''} = \sum_{m''} \pi_{D}^{t,m} \bar{\pi}_{WT}^{t,m'} & ,\forall t,m,m',m'' \\ \pi_{D}^{t,m} \epsilon\, \boldsymbol{\pi}_{D}^{t} & ,\forall m \\ \bar{\pi}_{WT}^{t,m'} \epsilon\, \bar{\boldsymbol{\pi}}_{WT}^{t} & ,\forall m' \\ \pi_{Dr}^{t,m''} \epsilon \boldsymbol{\pi}_{Dr}^{t} & ,\forall m'' \end{cases} \quad (26)$$

Obviously, the expected value of the residual demand (i.e. $P_{Dr}^{expt,t}$) can be formulated in (27).

$$P_{Dr}^{expt,t} = \sum_{m''} P_{Dr}^{t,m''} \pi_{Dr}^{t,m''} \quad ,\forall t \quad (27)$$

## III. Simulation and Numerical Results

In this section, the proposed framework is implemented on the modified IEEE 40-generator system to find out the optimal risk-oriented operation scheme for wind-thermal units integrated with CAES as well as WF power generation curtailing. Fig. 2 illustrates the modified test system, comprising 40 generators, four areas, and six transmission tie-lines. Other parameters of the test system and wind farms can be found in [10] and [23].

The test system is modified by installing two wind farms in area 2 and 3 with the capacity of 25% and 20% of the total installed capacity of thermal units in each zone, respectively, as well as two CAESs with the capacity of 400 MWh in these areas. Also, some other parameters used in the simulation are listed in TABLE I.

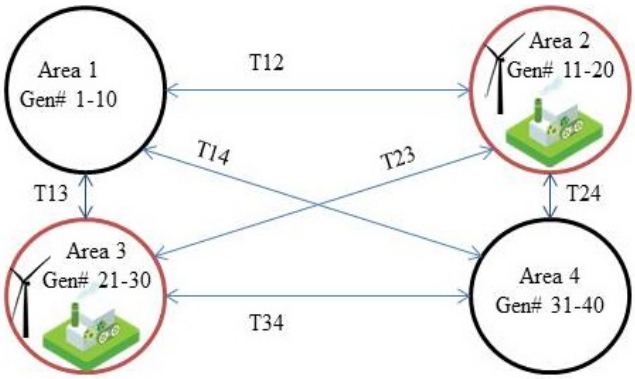


Fig. 2 The 40-generator IEEE test system integrated with WF & CAES

Furthermore, as the proposed strategy is a non-convex and non-linear problem with a large number of decision variables and constraints, an optimization approach using hybrid particle swarm optimization–shuffle frog leaping (PSO–SFL) algorithm is used [24]. All analyses are made in MATLAB software on a CORE i7 laptop machine with 2.4GHz 1GB RAM. The maximum number of iterations and populations are set to 100 and 200, respectively.

In order to demonstrate the impact of CAES and WF integration on the MAED, the results for the base case (original IEEE 40-generator system), the WF case (IEEE 40-generator system integrated with WF) and the modified WF & CAES case (IEEE 40-generator system integrated with WF & CAES) for different amount of risk (β) are tabulated in Table II for the 25% and 20% penetration levels of WF and CAES, respectively. The obtained results from Table II reveal that the operational cost in the modified WF & CAES case decreases by 7.2% for $\beta = 1$ in comparison with that of the base case, where, the risk function value is approximately 0.14% when $\beta = 1$. Moreover, the risk and operational cost functions are approximately 0.07% and $2,456,077, respectively, in case of $\beta = 0$. Furthermore, Table III presents different penetration levels of WF and CAES in the power system and their impacts on the operational cost, risk, and spinning reserves of thermal units and CAES. According to the results, the penetration increase of these units reduces the operational cost. However, there is no clear relationship between the WF and CAES penetration and operational risk.

TABLE I
Constant Parameters Used in the Simulations

| | |
|---|---|
| $\rho^{ch,k}$ | 0.85 |
| $\rho^{dis,k}$ | 0.90 |
| $\Psi^{dis,k}$ | 0.4185 |
| $\Psi^{s,k}$ | 0.837 |
| $\xi_{O\&M}^{w}$ | 3.973 ($/MWh) |
| $Vc_{Exp}^{k}, Vc_{Com}^{k}$ | 0.87 ($/kWh) |
| $\varphi_{NG}$ | 3.5 ($/GJ) |

TABLE II
Results Obtained for Three Cases & Different β

| Cases | Objective | Low risk (β=0) | Medium risk (β=0.5) | High risk (β=1) |
|---|---|---|---|---|
| Base Case | Cost ($) | N/A | N/A | 2,511,795 [10] |
| WF: 25% | Cost ($) | 2,494,592 | 2,387,918 | 2,369,615 |
| | Risk (%) | 0.103 | 0.156978 | 0.2843131 |
| WF: 25% and 20% CAES: 400 MWh | Cost ($) | 2,456,077 | 2,379,807 | 2,331,637 |
| | Risk (%) | 0.0706 | 0.0986 | 0.1434 |

This article has been accepted for publication in a future issue of this journal, but has not been fully edited. Content may change prior to final publication. Citation information: DOI 10.1109/TSTE.2019.2931670, IEEE Transactions on Sustainable Energy



TABLE III
IMPACT OF DIFFERENT PENETRATION OF WF AND CAES

| Penetration | Obj. $ SR | Low risk (β=0) | Medium risk (β=0.5) | High risk (β=1) |
|---|---|---|---|---|
| WF: 20% and 15% CAES: 300 MWh | Cost ($) | 2,471,911 | 2,408,637 | 2,365,783 |
| | Risk (%) | 0.0796 | 0.1017 | 0.1972 |
| | $SR_{TU}$ (MWh) | 129,940 | 125,450 | 125,260 |
| | $SR_{CAES}$ (MWh) | 6,438 | 6,356 | 6,344 |
| WF: 25% and 20% CAES: 400 MWh | Cost ($) | 2,456,077 | 2,379,807 | 2,331,637 |
| | Risk (%) | 0.0706 | 0.0986 | 0.1434 |
| | $SR_{TU}$ (MWh) | 131,499 | 129,540 | 127,567 |
| | $SR_{CAES}$ (MWh) | 6,721 | 6,569 | 6,399 |
| WF: 30% and 25% CAES: 500 MWh | Cost ($) | 2,368,601 | 2,339,454 | 2,312,785 |
| | Risk (%) | 0.0575 | 0.0671 | 0.1338 |
| | $SR_{TU}$ (MWh) | 135,439 | 132,711 | 132,139 |
| | $SR_{CAES}$ (MWh) | 7,499 | 7,509 | 7,198 |

It can be deduced that the higher penetration of WF increases the operational risk due to the intermittency of these units' generation. On the other hand, the participation of CAES can handle a portion of the WF power generation uncertainty as well as increasing the system spinning reserve. To summarize, the penetration level of WF and CAES have the opposite impact on the operational risk, while both of them reduce the cost.

Apparently, there is a conflict between these two objective functions. The value of objective functions for $\beta = 0.5$ is reported in Tables II and III for different cases. Moreover, Fig. 3 depicts the value of the two functions, operational cost and risk, for different amounts of risk ($\beta = 0, 05, 1$). As it is clear from this figure, the monotonically decreasing trend shows the conflict between these two objectives. Moreover, it is obvious that the CAES has a positive influence on both operational cost and risk. It can be stated that the presence of CAES in the power network improves the spinning reserve margin, and consequently further residual demand uncertainty would be confined within the up/down spinning reserve. According to the results from Table II, it is obvious that the operational risk is reduced in all cases for different amount of risk. The total wind power generation curtailment for different amounts of risk (β=0, 0.5, 1) is listed in Table IV for two cases (the WF case and the modified WF & CAES case).

According to the obtained results, it is clear that in the case of β=1, the total curtailment level is lower than the two other cases. It means that the WF power generation should be higher in order to decrease the operational cost because the operational cost of wind generations is negligible compared to costs associated with thermal units. Conversely, the higher level of WF curtailment in the case of $\beta = 0$, the higher thermal unit generations, leading to the lower operational risk. The total value of curtailment level in the both cases (the WF case and the modified WF & CAES case) for β=0.5 lies between the total curtailment level for β=0 and β=1. In result, the power system decision maker is able to make an appropriate trade-off between the operational cost and operational risk via considering β=0.5.

Moreover, according to the results from this table, the WF power generation curtailment level decreases in the presence of CAES in comparison to the case integrated with WF only. In other words, the CAES units are able to manage the uncertainty of WF generation with their ability of storing the extra WF power generation rather than curtailing them.

To sum up, CAES units are able to reduce the operational cost in two ways, decreasing the curtailment level in order to increase the participation of WF in meeting demand, and being charged during off-peak as well as discharged in peak hours. Results from Tables II-IV supports these statements.

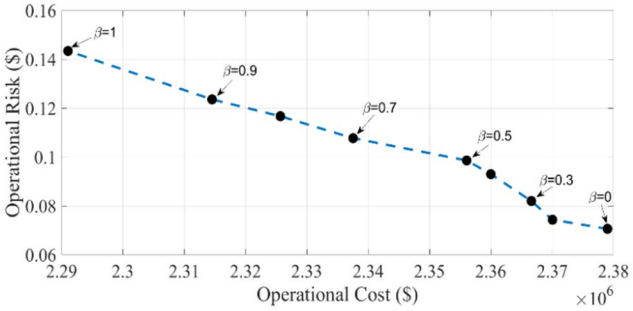


Fig. 3 Operational cost and risk with respect to different β

TABLE IV
WF POWER CURTAILMENT LEVEL WITH RESPECT TO DIFFERENT β

| Case | Low risk (β=0) | | Medium risk (β=0.5) | | High risk (β=1) | |
|---|---|---|---|---|---|---|
| | Area2 ($C^{1,t}$) | Area3 ($C^{2,t}$) | Area2 ($C^{1,t}$) | Area3 ($C^{2,t}$) | Area2 ($C^{1,t}$) | Area3 ($C^{2,t}$) |
| WF | 112 | 113 | 106 | 112 | 105 | 95 |
| WF& CAES | 96 | 76 | 81 | 72 | 49 | 44 |

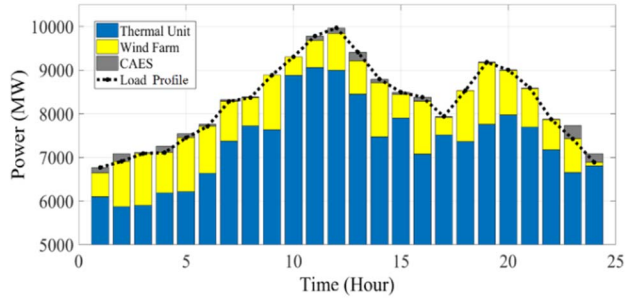


Low risk ($\beta = 0$)

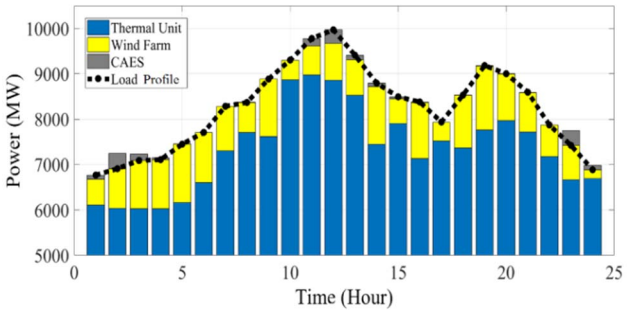


Medium risk ($\beta = 0.5$)

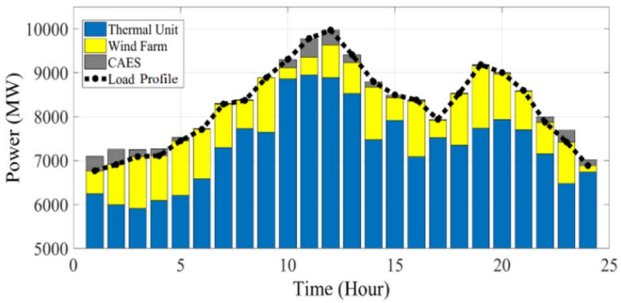


High risk ($\beta = 1$)

Fig. 4 Share of power generations for different values of β

This article has been accepted for publication in a future issue of this journal, but has not been fully edited. Content may change prior to final publication. Citation information: DOI 10.1109/TSTE.2019.2931670, IEEE Transactions on Sustainable Energy



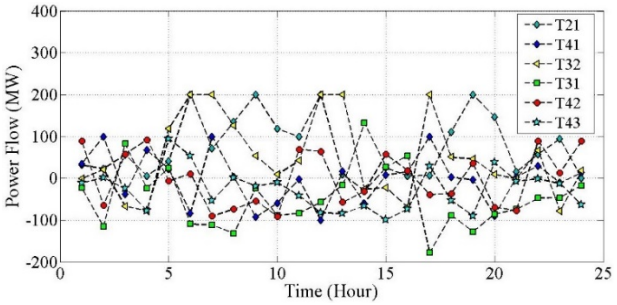


Fig. 5 The power flow (MW) related to the tie-lines for $\beta = 0.5$

The share of thermal units, WFs and CAESs in meeting the required demand is depicted in Fig. 4Fig. 4 for three different amount of risk. Accordingly, the total contributions of thermal units are 176,674 MWh, 176,436 MWh and 176,192 MWh for $\beta = 0$, $\beta = 0.5$ and $\beta = 1$, respectively; while the WF generation for these cases is 21,922 MWh, 22,103 MWh and 22,392 MWh, respectively. Clearly, the contribution of thermal units markedly decreases as the value of $\beta$ grows, while the situation for WF generations is the opposite. Moreover, the charging/discharging control of CAES is demonstrated as well. As expected, the CAES units charge during off-peak and discharge during peak demand for all three different cases. In addition, the concept of CAES utilization is to compensate the risk associated with WF. Therefore, in low risk situation, CAES utilization decreases.

The power exchange between different areas and the tie-lines is one of the most important constraints for operators which should be satisfied [25]. Apparently, the power flow in tie-lines are different as $\beta$ changes, meaning that the energy transactions through area-connecting lines would change according to the importance weight of the risk function. Fig. 5 illustrates the power flow related to the tie-lines in the case of $\beta = 0.5$. According to this figure, it can be observed that the power flow through the tie-lines are confined within their permitted level. In addition, Fig. 6 and Fig. 7 give more information of the simulation for $\beta = 0.5$. The proposed risk index as well as the hourly spinning reserve curve supplied by both thermal units and CAESs are shown in Fig. 6. The risk index increases during peak demand, and in some off-peak hours (i.e. hour#1, 24) as well, because of the increasing rate of CAES charging. However, during the shoulder period, the risk index is low. Also, it can be seen that the spinning reserve shows the opposite trend.

By increasing the amount of spinning reserve, the risk index decreases, implying that the probability of expected residual demand ($P_{Dr}^{expt,t}$) falls within the available up/down spinning reserve. Also, the costs associated with thermal units and the monetary profit obtained by CAESs are depicted in Fig. 7. Based on this figure, the thermal units' cost tracks the demand variation, because of the high proportion of these units in power generation. The CAES operational cost in some peak hours is negative, which means the CAES units inject power to the system in order to meet the demand. While in some off-peak hours it is positive, it means these units are charged in these hours and buy power from the grid. The proposed method can be easily expanded for a longer period of time efficiently using the forward-backward approach in [26].

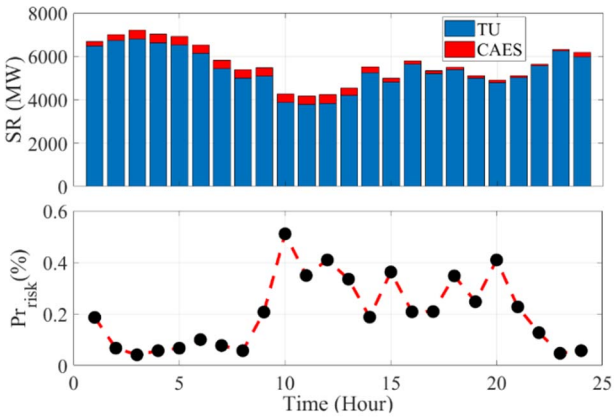


Fig. 6 Scheduled system up spinning reserve (SR) and the daily risk index for $\beta = 0.5$

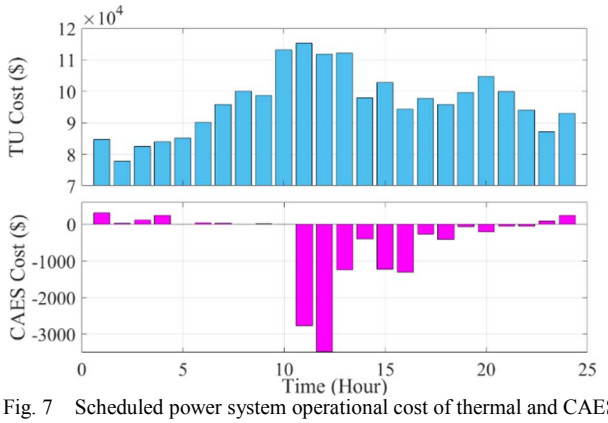


Fig. 7 Scheduled power system operational cost of thermal and CAES units for $\beta$=0.5

## IV. Conclusion

In this paper, a probabilistic model for MAED is proposed in which CAES units are incorporated with wind-thermal units to satisfy the demand. The proposed model takes advantage of CAES and intentional wind generation curtailment to present an optimal strategy desirable for system operators in the presence of load and wind fluctuations. To serve this purpose, a risk-based model is developed to consider the possibility of providing spinning reserve by CAES next to conventional thermal units, in the context of single outage of thermal units. The model simultaneously deals with the operational cost and risk functions by adjusting their weight parameters ($\beta$) through the used weighted sum method. By conducting the proposed method on a large-scale case study, it is shown that incorporating CAES in the MAED can effectively improve the spinning reserve capacity, which, in turn, leads to lower operational cost. Furthermore, the obtained results demonstrate that using the proposed strategy for wind curtailment through controlling the blade pitch angle has a positive impact on the reduction of the presented risk concept.

## References

[1] H. Safaei, D. W. Keith, and R. J. Hugo, "Compressed air energy storage (CAES) with compressors distributed at heat loads to enable waste heat utilization," *Applied Energy,* vol. 103, pp. 165-179, 2013/03/01/ 2013.

[2] N. S. Hasan, M. Y. Hassan, H. Abdullah, H. A. Rahman, W. Z. W. Omar, and N. Rosmin, "Improving power grid performance using parallel connected Compressed Air Energy Storage and wind turbine system," *Renewable Energy,* vol. 96, pp. 498-508, 2016/10/01/ 2016.

[3] H. Safaei and D. W. Keith, "Compressed air energy storage with waste heat export: An Alberta case study," *Energy Conversion and Management,* vol. 78, pp. 114-124, 2014/02/01/ 2014.

[4] M. Abbaspour, M. Satkin, B. Mohammadi-Ivatloo, F. Hoseinzadeh Lotfi, and Y. Noorollahi, "Optimal operation scheduling of wind power integrated with compressed air energy storage (CAES)," *Renewable Energy,* vol. 51, pp. 53-59, 2013/03/01/ 2013.

[5] S. Shafiee, H. Zareipour, and A. M. Knight, "Considering Thermodynamic Characteristics of a CAES Facility in Self-Scheduling in Energy and Reserve Markets," *IEEE Transactions on Smart Grid,* vol. 9, pp. 3476-3485, 2018.

[6] A. Mohammadi, M. H. Ahmadi, M. Bidi, F. Joda, A. Valero, and S. Uson, "Exergy analysis of a Combined Cooling, Heating and Power system integrated with wind turbine and compressed air energy storage system," *Energy Conversion and Management,* vol. 131, pp. 69-78, 2017/01/01/ 2017.

[7] A. N. Ghalelou, A. P. Fakhri, S. Nojavan, M. Majidi, and H. Hatami, "A stochastic self-scheduling program for compressed air energy storage (CAES) of renewable energy sources (RESs) based on a demand response mechanism," *Energy Conversion and Management,* vol. 120, pp. 388-396, 2016/07/15/ 2016.

[8] D. C. Secui, "Large-scale multi-area economic/emission dispatch based on a new symbiotic organisms search algorithm," *Energy Conversion and Management,* vol. 154, pp. 203-223, 2017/12/15/ 2017.

[9] H. Narimani, S.-E. Razavi, A. Azizivahed, E. Naderi, M. Fathi, M. H. Ataei*, et al.*, "A multi-objective framework for multi-area economic emission dispatch," *Energy,* vol. 154, pp. 126-142, 2018/07/01/ 2018.

[10] M. Basu, "Quasi-oppositional group search optimization for multi-area dynamic economic dispatch," *International Journal of Electrical Power & Energy Systems,* vol. 78, pp. 356-367, 2016/06/01/ 2016.

[11] G. Liu and K. Tomsovic, "Quantifying Spinning Reserve in Systems With Significant Wind Power Penetration," *IEEE Transactions on Power* Systems*,* vol. 27, pp. 2385-2393, 2012.

[12] H. Daneshi and A. K. Srivastava, "Security-constrained unit commitment with wind generation and compressed air energy storage," *IET Generation, Transmission & Distribution,* vol. 6, pp. 167-175, 2012.

[13] A. Arefi, A. Abeygunawardana, and G. Ledwich, "A New Risk-Managed Planning of Electric Distribution Network Incorporating Customer Engagement and Temporary Solutions," *IEEE Transactions on Sustainable Energy,* vol. 7, pp. 1646-1661, 2016.

[14] R. Entriken, P. Varaiya, F. Wu, J. Bialek, C. Dent, A. Tuohy*, et al.*, "Risk Limiting Dispatch," in *2012 IEEE Power and Energy Society General Meeting*, 2012, pp. 1-5.

[15] N. Zhang, C. Kang, Q. Xia, Y. Ding, Y. Huang, R. Sun*, et al.*, "A Convex Model of Risk-Based Unit Commitment for Day-Ahead Market Clearing Considering Wind Power Uncertainty," *IEEE Transactions on* Power *Systems,* vol. 30, pp. 1582-1592, 2015.

[16] F. Bavafa, T. Niknam, R. Azizipanah-Abarghooee, and V. Terzija, "A New Biobjective Probabilistic Risk-Based Wind-Thermal Unit Commitment Using Heuristic Techniques," *IEEE Transactions on Industrial Informatics,* vol. 13, pp. 115-124, 2017.

[17] P. Aliasghari, M. Zamani-Gargari, and B. Mohammadi-Ivatloo, "Look-ahead risk-constrained scheduling of wind power integrated system with compressed air energy storage (CAES) plant," *Energy,* vol. 160, pp. 668-677, 2018/10/01/ 2018.

[18] S. Shafiee, H. Zareipour, A. M. Knight, N. Amjady, and B. Mohammadi-Ivatloo, "Risk-Constrained Bidding and Offering Strategy for a Merchant Compressed Air Energy Storage Plant," *IEEE Transactions* on *Power Systems,* vol. 32, pp. 946-957, 2017.

[19] J. F. Restrepo and F. D. Galiana, "Assessing the Yearly Impact of Wind Power Through a New Hybrid Deterministic/Stochastic Unit Commitment," *IEEE Transactions on Power Systems,* vol. 26, pp. 401-410, 2011.

[20] S. G. Jirsaraie, M. J. Ghadi, A. A. Vahed, J. Aghaei, L. Li, and J. Zhang, "Risk-Constrained Bidding Strategy for a Joint Operation of Wind Power and Compressed Air Energy Storage Aggregators," *IEEE Transactions on Sustainable Energy,* pp. 1-1, 2019.

[21] Y. Li, S. Miao, B. Yin, W. Yang, S. Zhang, X. Luo*, et al.*, *A real-time dispatch model of CAES with considering the part-load characteristics and the power regulation uncertainty* vol. 105, 2019.

[22] V. V. Petrov, "Limit theorems of probability theory: sequences of independent random variables," Oxford, New York1995.

[23] (2015). *"Ontario power authority database"*. Available: http:// www.powerauthority.on.ca

[24] M. Gitizadeh, A. A. Vahed, and J. Aghaei, "Multistage distribution system expansion planning considering distributed generation using hybrid evolutionary algorithms," *Applied Energy,* vol. 101, pp. 655-666, 2013/01/01/ 2013.

[25] H. Pezeshki, A. Arefi, G. Ledwich, and P. Wolfs, "Probabilistic Voltage Management Using OLTC and dSTATCOM in Distribution Networks," *IEEE Transactions on Power Delivery,* vol. 33, pp. 570-580, 2018.

[26] A. Abeygunawardana, A. Arefi, and G. Ledwich, "An efficient forward-backward algorithm to MSDEPP including batteries and voltage control devices," in *2014 IEEE PES General Meeting | Conference & Exposition*, 2014, pp. 1-5.

**Ali Azizivahed** received the M.Sc. degree from Shiraz University of Technology, Shiraz, Iran, in 2012, in power electrical engineering. He is currently pursuing the Ph.D. degree in electrical engineering at the University of Technology Sydney, Sydney, Australia.

**Seyed-Ehsan Razavi** received the M.S. degree from University of Birjand, Birjand, Iran, in 2013, in electrical engineering. He is currently pursuing the Ph.D. degree in electrical engineering at the Murdoch University, Perth, Australia.

**Ali Arefi** (M'11–SM'14) received the Ph.D. degree in electrical engineering in 2011. Since 2015, he has been a Senior Lecturer with the Discipline of Engineering and Energy, Murdoch University, Perth, Australia.

**Mojtaba Jabbari Ghadi** is pursuing the Ph.D. degree in electrical engineering at the University of Technology Sydney, Australia, since 2017.

**Li Li** received his Ph.D. degree from University of California, Los Angeles in 2005. He joined University of Technology Sydney, in 2011, and currently he is an Associate Professor.

**Jiangfeng Zhang** received his PhD in Computing Mathematics from Xi'an Jiaotong University, China, and also a PhD in Electronic and Electrical Engineering from the University of Strathclyde, UK. He is currently a senior lecturer at the University of Technology Sydney.

**Miadreza Shafie-khah** (M'13-SM'17) received the Ph.D. degree in electrical engineering from Tarbiat Modares University, Tehran, Iran, in 2012. Currently, he is an Assistant Professor at the University of Vaasa, Vaasa, Finland.

**João P. S. Catalão** (M'04-SM'12) received the Ph.D. degree and Habilitation for Full Professor ("Agregação") from the University of Beira Interior (UBI), Covilha, Portugal, in 2007 and 2013, respectively. Currently, he is a Professor at the Faculty of Engineering of the University of Porto (FEUP), Porto, Portugal, and Research Coordinator at INESC TEC.